Scaling of T_c in proximity-coupled superconducting/normal-metal multilayers

M. L. Wilson and J. A. Cowen
Department of Physics and Astronomy, Michigan State University, East Lansing, Michigan 48824
(Received 24 March 1993)

The superconducting transition temperature T_c has been measured in the multilayered system Nb/CuX, where CuX represents Cu, $Cu_{1-y}Mn_y$, or $Cu_{0.95}Ge_{0.05}$. The advantage of this system is that the superconductor layer thickness, normal-metal layer thickness, normal-metal magnetic concentration, and normal-metal bulk resistivity can be independently varied. Our data show that the variation of T_c with changing superconductor-layer thickness d_s exhibits scaling consistent with the equation $(T_c^b - T_c)/T_c^b = (d_s/d_0)^{-p}$, where d_0 is a fitting parameter and T_c^b is T_c for bulk Nb. We find the exponent p to increase systematically with increasing normal-metal layer thickness, and magnetic impurity concentration, with $1 \le p < 2$, consistent with the limiting forms of two theoretical models.

I. INTRODUCTION

Superconductor/normal-metal (S/N) and superconductor/insulator (S/I) multilayers are of current interest both because of their intrinsic physics and their ability to simulate phenomena occurring in high-T_c superconductors (HTSC's).[1] The advantage of multilayers over HTSC compounds is that the S and N layer thicknesses and S and N materials can be independently varied, while in HTSC's the layer thicknesses and materials are fixed for each compound. Another regime of study open to multilayers is the mutual coexistence of magnetic and superconducting order. Using ferromagnetic,[2] antiferromagnetic,[3] or spin-glass[4] N layers, it is possible to tune the magnetic and superconducting ordering temperatures T_f and T_c, respectively, such that $T_f < T_c$ or $T_f > T_c$. In this manner a greater understanding of the interplay between magnetic and superconductive ordering is possible.

The superconducting properties of S/N multilayers are dominated by a proximity-induced superconducting pair density penetrating into the normal layer. This N layer pair density leads to a renormalization of the pair density in S and also mediates superconducting coupling between S layers.

We have analyzed the behavior of T_c for independent variation of d_s, d_n, the magnetic nature of N, and the electric mean free path ℓ_n of the N layer, in a single multilayer system Nb/CuX where CuX represents Cu, CuMn, or CuGe. Due to the large local moment of Mn in a Cu host ($S_{Mn} = \frac{5}{2}$), one can shift smoothly from the nonmagnetic to the strongly magnetic limit by increasing y in $Cu_{1-y}Mn_y$ alloys. Increasing y, however, also leads to a decrease in ℓ_n. To correct for mean-free-path induced changes in the T_c's of Nb/CuMn samples, our results are compared with T_c's obtained in Nb/CuGe samples. In a Cu host, Ge impurities are nonmagnetic and lead to roughly the same decrease in ℓ_n with impurity concentration as occurs in CuMn alloys.[5] Therefore CuGe layers should correctly model changes in T_c due to changes in ℓ_n.

We begin in Sec. II with a discussion of sample fabrication and characterization. Section III contains the experimental results for the dependence of T_c on d_n, d_s, y, and ℓ_n. These results are then compared with the predictions of two theoretical models in Sec. IV. Finally, our results are summarized in Sec. V.

II. SAMPLE PREPARATION AND CHARACTERIZATION

Multilayer samples were prepared by dc sputtering onto polished, oxidized, single-crystal (001)-oriented Si substrates. Substrates were placed on a computer-controlled movable stage, and the nominal layer thicknesses were determined by the measured deposition rates and time the substrate spent over each sputtering target. During deposition the substrate temperature was maintained between $-20°$ and $+20$ °C at sputtering rates of typically 0.8 nm/sec for Nb and 1.0 nm/sec for CuX. Before sputtering the chamber was pumped to less than 2×10^{-8} torr, then backfilled with ultra-high-purity Ar to a pressure of $\sim 2.5\times10^{-3}$ torr. Additional details of the sputtering system are given elsewhere.[6]

Sputtering targets of 3-9's Nb and 6-9's Cu were obtained from Angstrom Sciences.[7] We fabricated the CuMn and CuGe alloy targets from starting materials consisting of 6-9's Cu, 4-9's Mn and 6-9's Ge obtained from Aesar.[8] The materials were placed in a crucible of boron-nitride-lined graphite and heated in an rf induction furnance under ~ 250 torr of a 90% Ar/10% H_2 gas mixture.

The Mn or Ge concentrations in the CuX alloys were determined by magnetization and energy dispersive x-ray (EDX) measurements. $Cu_{1-y}Mn_y$ is a spin glass exhibiting a peak in its temperature-dependent magnetization at a spin-freezing transition temperature T_f which is directly related to y.[9] The nominal values of y in the CuMn alloys were obtained from T_f's measured on 500 nm-thick sputtered films.

EDX measures elemental compositions by exciting a sample with a high-energy electron beam and comparing

0163-1829/94/49(9)/6228(6)/$06.00

the relative fluorescent x-ray line intensities from the host Cu and impurity atoms Mn or Ge. These intensities are suitably normalized and compared with those expected from each pure material. For CuMn alloys with $y > 0.010$, magnetization and EDX measurements agree to within 10%. Larger disagreements are observed at low y due to the increased difficulty of quantitative x-ray peak detection. For CuGe alloys, EDX data provide the only measure of Ge concentration, which was 4.9 ± 0.3 at. % for the target used in these experiments. EDX data also show no evidence for any other impurities present in our films above the detection limit of the method (~ 0.1 at. %).

X-ray diffraction scans taken with the scattering vector normal to the film plane were used to extract information about the individual layer structure, the multilayer periodicity, and rms deviations in the thickness of each layer. The Nb and CuX layers crystallize in their bulk structures, bcc Nb and fcc CuX with their densest packed atomic planes, Nb(110) and CuX(111), parallel to the film plane. For thick layers, first- and second-order Bragg peaks are observed due to scattering from the Nb(110) and CuX(111) planes, as shown in Fig. 1(a) for a $Nb/Cu_{0.997}Mn_{0.003}$ 70 nm/70 nm multilayer. As d_s and d_n decrease, additional peaks appear due to the bilayer periodicity, $\Lambda = d_s + d_n$. These new peaks appear as satellites of the Bragg peaks and obey Bragg's law $[n\lambda = 2\Lambda \sin(\theta)]$ with characteristic distance Λ, as illustrated in Fig. 1(b) for a $Nb/Cu_{0.997}Mn_{0.003}$ 13.0 nm/10.0 nm multilayer. Satellites are typically observed for $\Lambda \leq 30$ nm. Bilayer thicknesses determined from these satellites are within 5% of those calculated from the sputtering conditions.

The Nb and CuX lattice parameters can be readily measured by analyzing the peak positions of the Nb(110) and CuX(111) peaks. No change in either lattice spacing is observed for $\Lambda \geq 15$ nm (Fig. 1). As Λ decreases below about 15 nm, the satellite structure begins to obscure the Nb(110) and CuX(111) peaks, as shown in Fig. 2(a) for a Nb/Cu 3.0 nm/2.0 nm multilayer. However, for small Λ, the second-order Nb and CuX Bragg peaks remain well

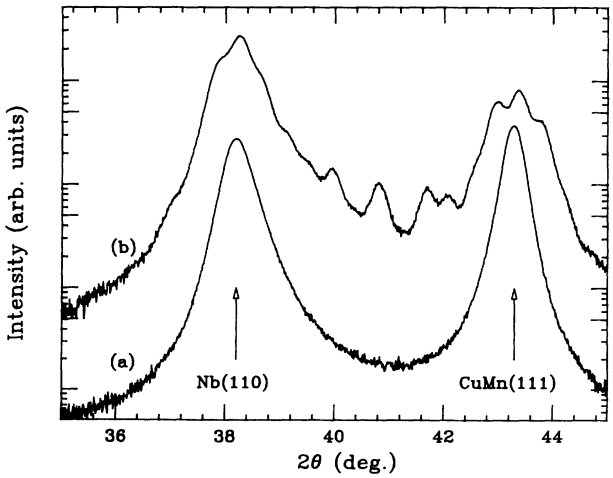

FIG. 1. X-ray diffraction scans for $Nb/Cu_{0.997}Mn_{0.003}$. (a) 70.0 nm/70.0 nm and (b) 13.0 nm-10.0 nm multilayers.

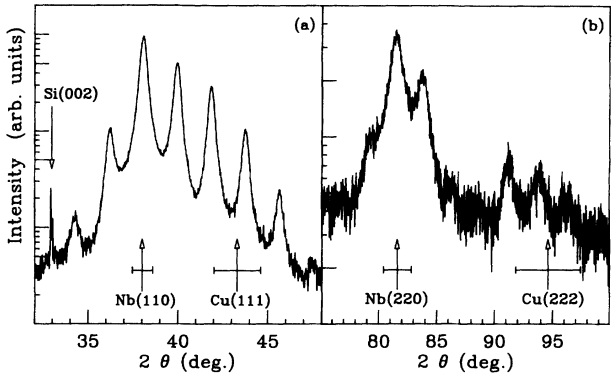

FIG. 2. X-ray diffraction scans for Nb/Cu multilayers about the (a) first- and (b) second-order Nb(110) and Cu(111) peaks for a Nb/Cu 3.0 nm/2.0 nm sample. Arrows and horizontal bars denote the bulk Nb lattice spacing $\pm 1.5\%$ and the bulk Cu lattice spacing $\pm 3\%$.

resolved, allowing an accurate measure of the Nb and CuX lattice spacings to be obtained [Fig. 2(b)]. Based upon these peak positions, we find that the Nb lattice parameter remains within 1.5% of its bulk value for $d_s > 3.0$ nm and that the CuX lattice parameter remains within roughly 3% of its bulk value for $d_n > 2.0$ nm. In addition, extended x-ray absorption fine structure (EXAFS) examinations of the Cu K-edge in Nb/CuX multilayers indicate no more than a 1% change in the CuX lattice parameter down to 2.0 nm of CuX,[10] in agreement with the x-ray diffraction results.

Recently, Fullerton *et al.*[11] developed a recursive x-ray diffraction modeling program to study layer thickness fluctuations in Nb/Cu multilayers. Their analysis of sputtered Nb/Cu 2.6 nm/2.0 nm multilayers shows that experimental observation of satellites associated with the Nb(220) and Cu(222) peaks places an upper limit of 0.3 nm on the rms fluctuations of the two layer thicknesses. From the similarity in layer thicknesses and satellite structure of our Nb/Cu 3.0 nm/2.0 nm multilayer and those of Fullerton *et al.*, we infer that the rms fluctuations of d_s and d_n in our sample are less than or of order 0.3 nm. We have observed satellites near the Nb(220) and CuX(222) peaks in samples with $d_s \leq 6.0$ nm and $d_n \leq 5.0$ nm, indicating no serious difference in the magnitude of layer thickness fluctuations for multilayers with d_s and d_n larger than those of the Nb/Cu 3.0 nm/2.0 nm sample. This indicates very uniform layering with little variation in d_n or d_s throughout our samples.

To summarize, the samples consist of polycrystalline bcc Nb and fcc CuX layers with the Nb(110) and CuX(111) planes parallel to the substrate and lattice spacings consistent with those of the separate bulk materials. Bilayer thickness measurements agree with those expected from the sputtering conditions, while the small rms thickness fluctuations imply that d_s and d_n are uniform throughout our samples. We conclude that, as d_s and d_n

are reduced, no structural changes are observed that might influence the superconducting properties.

III. EXPERIMENTAL RESULTS AND INTERPRETATION

T_c was determined from 4-probe resistive measurements on patterned samples. Samples were patterned by sputtering each multilayer through a stainless steel mask in physical contact with the substrate. This procedure produced samples with rather broad edges, however, measurements on codeposited patterned and unpatterned samples showed no difference in T_c.

Measurements were made using a Quantum Design MPMS2 both as a cryostat and for computer control of a Keithley K181 nanovoltmeter and a K224 current source. The temperature accuracy and stability of this system is about 5 mK at temperatures near 6 K and somewhat better below 4 K. T_c was defined as the temperature at which the resistivity had reached 50% of its normal-state value. Typically, the widths of the resistive transitions (measured from 90% to 10% of the normal-state value) were less than 60 mK in a residual field of a few gauss. The bulk transition temperature of Nb, T_c^b, measured on 500 nm thick sputtered films, was 9.0 K with a sample to sample variation of ± 0.10 K. Based on the width, temperature accuracy, and sample reproducibility, the error in T_c was estimated to be ± 0.1 K. Although this error is small over most of the range of our data, it leads to rather larger fractional errors in the deviation of T_c from T_c^b when T_c is very near T_c^b.

The dependence of T_c on d_n for fixed d_s yields direct information about the behavior of superconducting electrons in the N layers. For small d_n, the superconducting pair density in N is large, leading to strong superconductive coupling between S layers and $T_c \simeq T_c^b$. As d_n is increased T_c decreases monotonically due to a reduction in the probability for paired electrons to traverse the N layer. Eventually, for very large d_n, the S layers are entirely decoupled from one another and T_c approaches a minimum value, T_c^m. Therefore, d_n^*, the value of d_n beyond which $T_c \simeq T_c^m$, is representative of the penetration depth of superconducting electrons into the N layer.

Figure 3 shows the dependence of T_c on d_n for a series of multilayers with fixed Nb thickness (28.0 nm) and Cu, $Cu_{0.95}Ge_{0.05}$, or $Cu_{1-y}Mn_y$ interlayers with 2 nm $\leq d_n \leq 600$ nm, and $0.003 < y \leq 0.022$. All samples exhibit a decrease of T_c with increasing d_n consistent with decreasing superconductive coupling. For thin nonmagnetic layers, T_c is independent of whether Cu or $Cu_{0.95}Ge_{0.05}$ layers are used, while for thick nonmagnetic layers ($d_n > 20$ nm), T_c increases on changing to $Cu_{0.95}Ge_{0.05}$ layers from Cu layers. Associated with this increase in T_c is a decrease in d_n^*. $Nb/Cu_{1-y}Mn_y$ multilayers exhibit the same trend of decreasing T_c with increasing d_n; however, in Nb/CuMn, T_c^m drops sharply on changing from Cu to $Cu_{0.997}Mn_{0.003}$ layers, but does not change significantly with further increases in y.

These trends yield qualitative information about the dominant scattering processes occurring in each of our

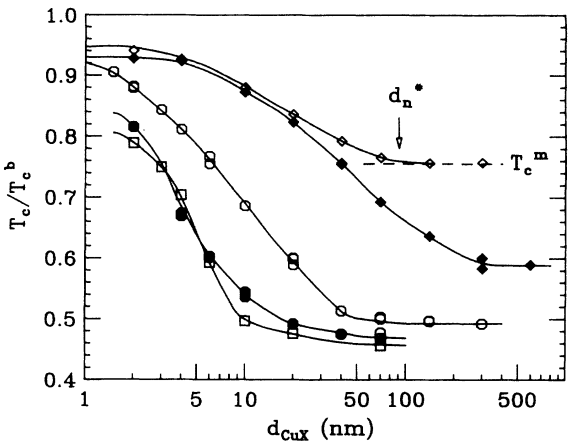

FIG. 3. Normalized superconducting transition temperature T_c/T_c^b as a function of the CuX layer thickness d_{CuX} for Nb/CuX multilayers having $d_s = 28.0$ nm. CuX materials are ◇, $Cu_{0.95}Ge_{0.05}$; ◆, Cu; ○, $Cu_{0.003}Mn_{0.003}$; ●, $Cu_{0.99}Mn_{0.01}$; □, $Cu_{0.978}Mn_{0.022}$. d_n^* and T_c^m for the Nb/CuGe series are shown. Solid lines are to guide the eye.

three N-layer materials. In a bulk superconductor, increasing the concentration of scatterers, decreases ℓ_s, increasing the rate at which superconducting electrons are scattered. For scattering from nonmagnetic impurities, these events are predominantly elastic and are non-pair-breaking. In a multilayered system, increasing the elastic scattering in N increases the probability that superconducting electrons are randomly scattered back into the S layer. This increased back-scattering rate reduces d_n^*, weakening the coupling strength between S layers while increasing the pair density in S, thereby increasing T_c. This is precisely the behavior observed for changing the N layer from Cu to $Cu_{0.95}Ge_{0.05}$.

For thin nonmagnetic N layers, however, T_c shows no increase on adding Ge. In thin films ℓ_n is limited by scattering from the S-N interfaces rather than by the impurity concentration. For these thin N layers, ℓ_n is approximately

$$\frac{1}{\ell_n} \simeq \frac{1}{\beta \ell_n^0} + \frac{1}{d_n} , \tag{1}$$

where ℓ_n^0 is the bulk mean free path of N:

$$\ell_n^0 \simeq \frac{(\rho \ell)_n}{\rho_n^0} , \tag{2}$$

ρ_n^0 is the bulk resistivity of N, $(\rho\ell)_n$ is the finite-size correction to the resistivity, and β is a constant of order 3/8 for thin films.[12] For sufficiently small d_n interfacial scattering will always dominate the mean free path and T_c will become independent of ℓ_n^0.

Mn impurities, which can scatter elastically and inelastically, increase both the elastic back-scattering rate, and the probability that pairs are destroyed in N. When magnetic pair breaking dominates, T_c and the superconductive coupling strength will decrease with increasing y due to an increase in the probability that su-

perconducting pairs are destroyed as they enter N. For small d_n, T_c is observed to decrease rapidly with increasing y, hence pair breaking is the dominant scattering mechanism in these thin N layers. However, for $d_n > d_n^*$ and $y > 0.003$, T_c becomes nearly independent of y. This saturation of T_c^m in Nb/CuMn multilayers is still being investigated.

Whereas the dependence of T_c on d_n yielded information about coupling strength between layers and about N-layer scattering mechanisms, an examination of the dependence of T_c on d_s for fixed d_n enables us to study changes in the properties of the superconducting material (density of states, gap parameter, etc.) as its thickness is reduced.

The normalized transition temperature T_c/T_c^b is shown in Fig. 4 plotted against the superconducting layer thickness d_s for two strongly coupled ($d_n = 2.0$ nm $Cu_{0.95}Ge_{0.05}$ and $Cu_{0.997}Mn_{0.003}$) and two weakly coupled ($d_n = 300$ nm $Cu_{0.95}Ge_{0.05}$ and 70 nm $Cu_{0.997}Mn_{0.003}$) multilayered series. From this data we observe that T_c decreases with decreasing proximity effect coupling strength (i.e., increased d_n or y) for all d_s. Based on this graph, however, it is difficult to see if the various series conform to a universal functional form. In Fig. 5 we plot the deviation of T_c from T_c^b, $t \equiv (T_c^b - T_c)/T_c^b$, as a function of d_s for these four series. This graph shows that all four series can be scaled as

$$t = (d_s/d_0)^{-p}, \tag{3}$$

with $1 \le p < 2$. We find that all Nb/CuX series studied to date can be fit to this relation. Values for p and the scale factor d_0 for the series in Fig. 5 and others are listed in Table I.

Thin, nonmagnetic N interlayer series (2.0 nm of Cu or CuGe) are best fit to $p = 1$. As the nonmagnetic N-layer thickness is increased, p increases systematically reaching an average of 1.24 for samples with decoupled S layers. d_0, however, is always smaller when using thick CuGe interlayers since T_c is enhanced in Nb/CuGe multilayers. Thin $Cu_{1-y}Mn_y$ layered samples show p increasing systematically with increasing y and d_n. Sample series having thick CuMn layers, however, show that d_0 and p are roughly independent of y. This shows that T_c in the decoupled limit in Nb/CuMn multilayers is roughly independent of Mn concentration at all Nb thicknesses.

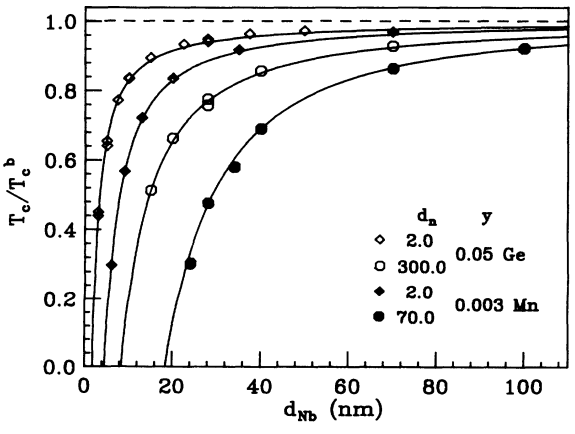

FIG. 4. Dependence of T_c/T_c^b on the Nb layer thickness d_s in Nb/$Cu_{1-y}Mn_y$ multilayers. The solid lines are fits to Eq. (3).

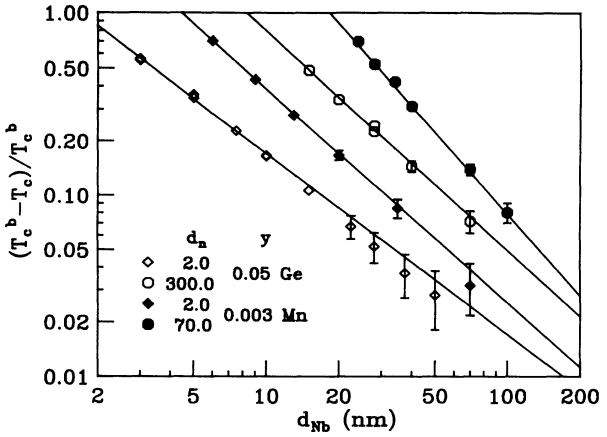

FIG. 5. Dependence of the reduced temperature $t = (T_c - T_c^b)/T_c^b$ on d_s in Nb/$Cu_{1-y}Mn_y$ multilayers. The solid lines are fits to Eq. (3).

To provide a check of Eq. (3) in the extremely magnetic limit we have reanalyzed data published by Wong *et al.*[2] on T_c in V/Fe multilayers and Fe/V/Fe sandwiches. We find that their data also scale according to relation (3).[13] In V/Fe multilayers, p increases rapidly with increasing ferromagnetic Fe thickness (i.e., decreased coupling), the data in Fe/V/Fe sandwiches, however, do not agree with either the V/Fe multilayer data or our Nb/CuX data. Wong *et al.* noted that for multilayers with thick Fe layers (approximately equal to those

TABLE I. Parameters obtained from fitting data to $t = (d_s/d_0)^{-p}$ with $t = (T_c - T_c^b)/T_c^b$. The parameters for V/Fe and Fe/V/Fe were obtained from fitting to data by Wong *et al.* (Refs. 2 and 13).

Interlayer	d_n	d_0	p
$Cu_{0.95}Ge_{0.05}$	2.0 nm	1.70±0.03	1.00±0.02
$Cu_{0.95}Ge_{0.05}$	300.0 nm	8.3±0.2	1.21±0.04
Cu	2.0 nm	1.76±0.04	0.98±0.02
Cu	300.0 nm	13.6±0.4	1.27±0.06
$Cu_{0.997}Mn_{0.003}$	2.0 nm	4.45±0.04	1.18±0.02
$Cu_{0.997}Mn_{0.003}$	20.0 nm	14.4±0.1	1.35±0.02
$Cu_{0.997}Mn_{0.003}$	70.0 nm	18.3±0.6	1.50±0.10
$Cu_{0.985}Mn_{0.015}$	2.0 nm	8.6±0.1	1.42±0.03
$Cu_{0.978}Mn_{0.022}$	2.0 nm	9.4±0.2	1.45±0.04
$Cu_{0.978}Mn_{0.022}$	70.0 nm	20.0±0.5	1.64±0.10
V/Fe	0.27 nm	13.1±0.1	1.26±0.02
V/Fe	0.41 nm	21.8±0.3	1.42±0.05
Fe/V/Fe	~5.0 nm	12.5±0.6	1.10±0.04

used in the sandwich films) T_c deviated from the trends observed using thin Fe layers. They proposed that the observed deviations at large d_{Fe} may be driven by a structural change but were unable to validate this proposal.

IV. THEORY

Most proximity effect models are derived using the dirty superconducting limit approximation: $\ell_i^0 \ll \xi_i^0$, where ℓ_i^0 is the bulk mean free path and ξ_i^0 is the clean limit value of the Pippard coherence length in material i. Two such models, valid for superconducting/magnetic-normal-metal multilayers, are those of Hauser, Theuerer, and Werthamer (HTW),[14] and Kaiser and Zuckermann (KZ).[15] In addition to the dirty limit, KZ also require that both layers be thin: $\ell_i^0 < d_i \ll \xi_i^0$.

Before applying these theories, the validity of using the dirty limit approximation must be established for our Nb and CuX layers, hence ℓ_i^0 and ξ_i^0 must be determined. To determine ℓ_i^0 we use the measured bulk resistivities of sputtered Nb and CuX samples in conjuction with Eq. (2)—these values are listed in Table II. ξ_{Nb}^0 is determined from the temperature dependence of the superconducting upper critical field near T_c in bulk sputtered Nb films—ξ_{Nb}^0 is also listed in Table II.

The normal metal coherence length cannot be directly measured, rather, it is estimated using the form of Kogan,[16]

$$\xi_n^0 = \frac{\pi\hbar k_b}{2e^2 T}\frac{1}{\gamma_n(\rho\ell)_n} . \tag{4}$$

Here, k_b is Boltzman's constant, $\hbar$ is Plank's constant, γ_n is the coefficient of the linear term in the specific heat, and $(\rho\ell)_n$ is the finite-size correction to the resistivity. The temperature T used in estimating ξ_n^0 is the highest temperature of physical interest, in our case T_c^b for Nb. To evaluate ξ_{CuX}^0 we assume there is no change in either γ or $(\rho\ell)$ due to the addition of the small Mn or Ge concentrations used in this study. With this assumption, and $\gamma_{Cu}=96.75$ J/m^{3}K (Ref. 17) and $(\rho\ell)_{Cu}=6.60\times10^{-16}$ Ω m^2,[12] we find $\xi_{CuX}^0 \simeq 160$ nm.

For all layer materials except pure Cu, the dirty superconducting limit approximation is valid at all layer thicknesses. For Cu layers, as d_{Cu} is reduced, ℓ_{Cu} becomes limited by interfacial scattering [Eq. (1)]. Hence, sufficiently thin Cu layers will also be governed by the dirty limit.

In terms of applicability to our data, the principal limits of interest are for thin nonmagnetic interlayers, where experimentally p is 1, and for thick strongly magnetic normal layers, where p increases to 1.64. In the thin, weakly magnetic limit, the HTW and KZ models collapse to

$$t_{HTW} \simeq \frac{\pi^2}{4}\frac{N_n(0)}{N_s(0)}\left[1+\frac{\tau_0}{\tau_s}\right]d_n d_s^{-1} \tag{5}$$

and

$$t_{KZ} \simeq \frac{N_n(0)}{N_s(0)}\left[\frac{\pi^2}{4}\frac{\Delta_b}{k_b T_c^b}g - \Psi\left[\frac{1}{2}\right]\right]d_n d_s^{-1} , \tag{6}$$

where $N_i(0)$ is the density of states at the Fermi level in i, Δ_b is the bulk gap parameter of S, $\Psi(\frac{1}{2})$ is the digamma function of $\frac{1}{2}$ [$\Psi(\frac{1}{2})=-1.964$], $\tau_0=\hbar/2\pi k_b T_c^b$, τ_s is the magnetic scattering time used by HTW, and g is the magnetic factor used by KZ.

These forms show that in the thin nonmagnetic limit, T_c should scale according to Eq. (3) with an exponent of -1. Values for d_0 predicted by these models, however, do not agree with those found experimentally. For the series having 2.0-nm-thick $Cu_{0.95}Ge_{0.05}$ layers, $d_0^{HTW} \simeq 1.17$ nm, $d_0^{KZ} \simeq 0.93$ nm, and $d_0^{Expt} = 1.70\pm0.03$ nm.[18]

For thick strongly magnetic N layers, KZ's model is not valid, however, HTW remains valid and collapses to

$$t_{HTW} \simeq \frac{\pi^2}{4}\frac{\hbar k_b}{6\pi e^2 T_c^b \gamma_s \rho_s^0} d_s^{-2} . \tag{7}$$

This leads to an effective value for d_0 of 40.2 nm. In this case, HTW predicts values for p and d_0 significantly larger than those found experimentally.

Previous work on Nb/Cu multilayers[19,20] and Nb films[21] have found that the data were best fit by the theories if the effective bulk T_c of Nb was depressed with decreased Nb thickness. This depression was related to lifetime broadening of the density of states caused by ℓ_{Nb} decreasing significantly with decreasing Nb thickness. Using these ideas, T_c^b is predicted to scale as

$$\frac{[T_c^{b,true} - T_c^b(d_s)]}{T_c^{b,true}} \propto d_s^{-1} , \tag{8}$$

where $T_c^{b,true}$ is the true bulk T_c of Nb and $T_c^b(d_s)$ is the thickness dependent T_c^b. Using this expression for T_c^b in Eq. (3) leads to an apparent reduction in the experimental values for d_0, with no significant change in p. Hence this process may explain the difference between the experimental and theoretical values for d_0.

TABLE II. Resistivities, mean free paths, and coherence lengths in Nb and CuX materials.

	Nb	Cu	$Cu_{0.997}Mn_{0.003}$	$Cu_{0.978}Mn_{0.022}$	$Cu_{0.95}Ge_{0.05}$	Units
ρ_i^0	7.2	0.5	3.4	9.4	19.4	$10^{-8}\Omega$ m
ℓ_i^0	4.4	130	19	7.0	3.4	nm
ξ_i	33	160	160	160	160	nm

V. CONCLUSIONS

The superconducting transition temperature in proximity coupled S/N multilayers displays a power-law dependence on the S-layer thickness. This form is found to hold for all N-layer thicknesses, mean free paths, and magnetic ion concentrations studied. In addition, the observed scaling law is predicted by the limiting forms of the HTW and KZ models. While the models appropriately predict the behavior of the scaling exponent, an effective depression of the bulk Nb T_c with decreasing d_{Nb} [consistent with lifetime broadening of $N_{Nb}(\omega)$] is required for the models to adequately predict values for the scale factor d_0.

ACKNOWLEDGMENTS

We would like to thank C. L. Foiles for useful discussions on the structural characterization of multilayers. This work was supported by the Center for Fundamental Materials Research and the NSF under Grant Nos. DMR-88-19429 and DMR-91-21481.

[1]W. R. White, A. Kapitulnik, and M. R. Beasley, Phys. Rev. Lett. **66**, 2826 (1991).

[2]H. K. Wong, H. Q. Yang, B. Y. Jin, Y. H. Shen, W. Z. Cao, and J. B. Ketterson, J. Appl. Phys. **55**, 2494 (1984); H. K. Wong, B. Y. Jin, H. Q. Yang, J. B. Ketterson, and J. E. Hilliard, J. Low Temp. Phys. **63**, 307 (1985).

[3]Y. Cheng and M. B. Stearns, J. Appl. Phys. **67**, 5038 (1990).

[4]M. L. Wilson, R. Loloee, and J. A. Cowen, Physica B **165-166**, 457 (1990).

[5]J. Bass, in *Metals: Electronic Transport Phenomena,* Vol. 15a of *Landolt-Börnstein Tables,* New Series Group III, edited by K. H. Hellwege (Springer-Verlag, Berlin, 1982), p. 177.

[6]J. M. Slaughter, W. P. Pratt, Jr., and P. A. Schroeder, Rev. Sci. Instrum. **60**, 127 (1989).

[7]Angstrom Sciences, P.O. Box 18116, Pittsburgh, PA 15236.

[8]Aesar/Johnson Matthey, P.O. Box 8247, Ward Hill, MA 01835-0747.

[9]K. H. Fischer, in *Metals: Electric Transport Phenomena,* Vol. 15a of *Landolt-Börnstein Tables,* New Series Group III, edited by K. H. Hellwege (Springer-Verlag, Berlin, 1982), p. 289.

[10]M. L. Wilson, and C. L. Foiles (unpublished).

[11]E. E. Fullerton, I. K. Schuller, H. Vanderstraeten, and Y. Bruynseraede, Phys. Rev. B **45**, 9292 (1992).

[12]J. Bass, in *Metals: Electronic Transport Phenomena,* Vol. 15a of *Landolt-Börnstein Tables,* New Series Group III, edited by K. H. Hellwege (Springer-Verlag, Berlin, 1982), p. 139.

[13]Wong *et al.*'s published data were of samples series of T_c vs d_{Fe} each at a fixed d_V. We have interpolated these data sets in order to extract the dependence of T_c vs d_V at fixed d_{Fe}.

[14]J. J. Hauser, H. C. Theuerer, and N. R. Werthamer, Phys. Rev. **142**, 118 (1966); **136**, A637 (1964).

[15]A. B. Kaiser and M. J. Zuckermann, Phys. Rev. B **1**, 229 (1970).

[16]V. G. Kogan, Phys. Rev. B **26**, 88 (1982).

[17]R. Hultgren, P. D. DeSai, D. T. Hawkins, M. Gleiser, K. K. Kelley, and D. D. Wagman, *Selected Values of the Thermodynamic Properties of the Elements* (American Society for Metals, Metals Park, OH, 1973).

[18]$N_i(0)$ from H. van Leuken, A. Lodder, and R. A. de Groot, J. Phys. Condens. Matter **3**, 7651 (1991).

[19]I. Bannerjee, Q. S. Yang, C. M. Falco, and I. K. Schuller, Solid State Commun. **41**, 805 (1982).

[20]P. R. Auvil and J. B. Ketterson, Solid State Commun. **67**, 1003 (1988).

[21]S. I. Park and T. H. Geballe, Physica **135B**, 108 (1985).